

The X-ray and radio-emitting plasma lobes of 4C23.56: further evidence of recurrent jet activity and high acceleration energies

Katherine M. Blundell¹ and A.C. Fabian²

¹University of Oxford, Astrophysics, Keble Road, Oxford OX1 3RH

²Institute of Astronomy, Madingley Road, Cambridge CB3 0HA

21 November 2018

ABSTRACT

New Chandra observations of the giant (~ 0.5 Mpc) radio galaxy 4C23.56 at $z = 2.5$ show X-rays in a linear structure aligned with its radio emission, but seemingly anti-correlated with the detailed radio structure. Consistent with the powerful, high- z giant radio galaxies we have studied previously, X-rays seem to be invariably found where the lobe plasma is oldest even where the radio emission has long since faded. The hotspot complexes seem to show structures resembling the double shock structure exhibited by the largest radio quasar 4C74.26, with the X-ray shock again being offset closer to the nucleus than the radio synchrotron shock. In the current paper, the offsets between these shocks are even larger, at ~ 35 kpc. Unusually for a classical double (FRII) radio source, there is smooth low surface-brightness radio emission associated with the regions *beyond* the hotspots (i.e. further away from the nucleus than the hotspots themselves), which seems to be symmetric for the ends of both jets. We consider possible explanations for this phenomenon, and reach the conclusion that it arises from high-energy electrons, recently accelerated in the nearby radio hotspots that are leaking into a pre-existing weakly-magnetized plasma that are symmetric relic lobes fed from a previous episode of jet activity. This contrasts with other manifestations of previous epochs of jet ejection in various examples of classical double radio sources namely (i) double-double radio galaxies by e.g. Schoenmakers et al, (ii) the double-double X-ray/radio galaxies by Laskar et al and (iii) the presence of a relic X-ray counter-jet in the prototypical classical double radio galaxy, Cygnus A by Steenbrugge et al. The occurrence, still more the prevalence, of multi-episodic jet activity in powerful radio galaxies and quasars indicates that they may have a longer lasting influence on the on-going structure formation processes in their environs than previously presumed.

Key words: galaxies: high-redshift, galaxies: jets, X-rays: individual (4C23.56)

1 INTRODUCTION

X-ray studies of classical double (FRII; Fanaroff & Riley 1974) radio galaxies and quasars seem — at significant distances out from their nuclei — to display two separate phenomena besides their compact, active galactic nuclei: the first of these is that considerable *extended* X-ray emission may be associated with the oldest parts of the lobes (e.g. Blundell et al. 2006; Johnson et al. 2007; Erlund et al. 2008a; Laskar et al. 2010). This is exemplified by our X-ray study of the powerful, giant, $z \sim 2$ radio galaxy 6C0905+39: our Chandra observations (Blundell et al. 2006) revealed that the *oldest* parts of the lobes (nearest to the nucleus, yet distinct from it) were predominantly where fairly smooth X-ray emission was detected even though the radio emission from that plasma (accelerated $> 10^8$ years ago when the hotspots were that close to the nucleus) had faded. This X-ray emission, extended over several 100 kpc, has been confirmed by subsequent, deeper XMM observa-

tions (Erlund et al. 2008a). It arises via inverse-Compton scattering of CMB photons (hereafter ICCMB) by the “spent” (i.e. relic) synchrotron particles having Lorentz factors of only $\gamma \sim 10^3$, too low to give synchrotron radiation detectable by current radio facilities (this requires rather higher Lorentz factors in the typical magnetic field strengths of aged lobe plasma). Where we detect ICCMB, this is a tracer of the $\gamma \sim 10^3$ particles; if these particles had been initially accelerated to higher energies then it is likely they would have *previously* radiated GHz-radio synchrotron before they lost significant amounts of their energy via expansion losses. An example of a relic radio source now observable only via ICCMB emission is HDF 130 at $z \sim 2$ (Fabian et al. 2009). As time goes by, even the ICCMB emission from relic lobes will fade and become undetectable with present X-ray instrumental capability (Mocz 2010).

The second phenomenon often revealed in powerful classical double radio sources is *compact* X-ray emission associated, though

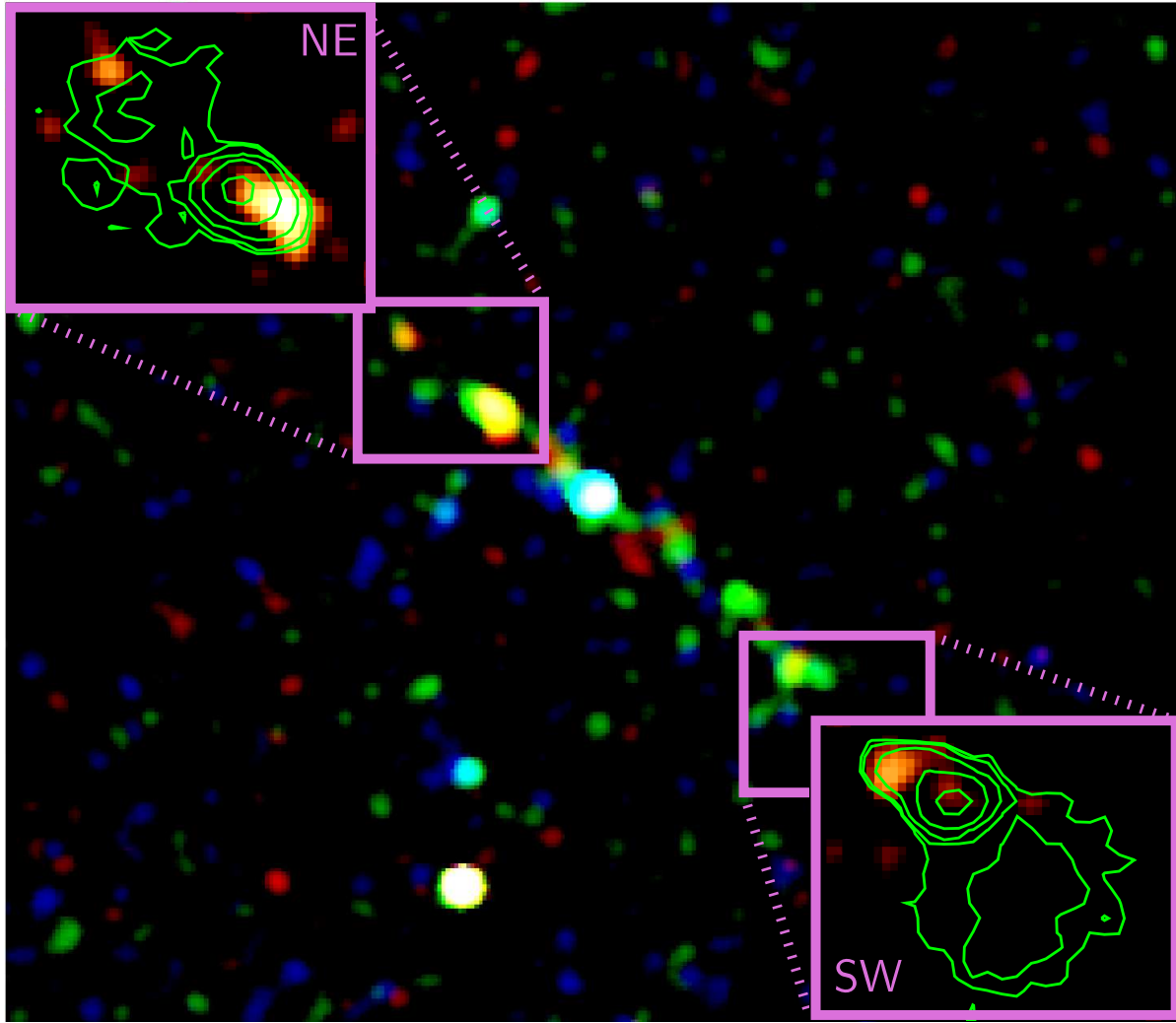


Figure 1. Smoothed Chandra image as colourscale showing that ICCMB X-rays are associated with the oldest parts of the lobe, *nearest* to the central nucleus (coloured white) though clearly resolved from it. A very similar picture was found from XMM observations (Johnson et al. 2007). Such ICCMB emission is a tracer of “spent” synchrotron particles: too lacking in energy to give synchrotron radiation at the usual radio wavelengths, but sufficiently energetic to upscatter CMB photons to become X-ray photons. As such this emission delineates the presence of $\gamma \sim 10^3$ particles. Red is soft and blue is hard. The green contours represent 5 GHz radio emission. The outermost extended radio regions external to the hotspots are considered in Sec 4. The regions inside the hotspots, towards the nucleus are referred to as the tails; these are resolved more clearly from the compact hotspots in the high-resolution 8 GHz image of Carilli et al. (1997, their fig. 35).

not co-spatial, with the radio hotspots. Angular resolution often presents a challenge to diagnosing the spatial separation of the compact X-ray shock structure from the compact radio shocks, but in the case of the giant nearby radio quasar 4C74.26, these are separated by a projected distance of 19 kpc (Erlund et al. 2010) while in 4C19.44 the separation is 14.5 kpc (Sambruna et al. 2002).

The particular object under study in this paper, 4C23.56, is a suitable target to further explore these two phenomena to try and discern what are their fundamental characteristics. 4C23.56 is a giant radio galaxy extending over 60 arcminutes, corresponding to 492 kpc projected on the plane of the Sky, previously studied in X-rays by Johnson et al. (2007).

Throughout this paper, all errors are quoted at 1σ unless otherwise stated and the cosmology is $H_0 = 71 \text{ km s}^{-1} \text{ Mpc}^{-1}$, $\Omega_0 = 1$ and $\Lambda_0 = 0.73$. One arcsecond represents 8.203 kpc on the plane of the sky at the redshift of 4C 23.56 of 2.48 (Roettgering et al.

1997) and the Galactic absorption along the line-of-sight towards this object is $1.29 \times 10^{21} \text{ cm}^{-2}$ (Dickey & Lockman 1990) but reported as $9.19 \times 10^{20} \text{ cm}^{-2}$ in the Leiden, Argentina, Bonn (LAB) survey (Kalberla et al. 2005).

2 DATA

2.1 New Chandra data

4C 23.56 was observed with Chandra ACIS-S for 91.69 ks on 2009 Aug 16–17. The data were taken in VFAINT mode and processed accordingly to improve background reduction. There were no significant background flares during the observation so the whole dataset was used. After background subtraction we detect 417 counts from the radio source in the 0.5–7 keV band, of which 256 are from the nucleus and 161 are from extended emission.

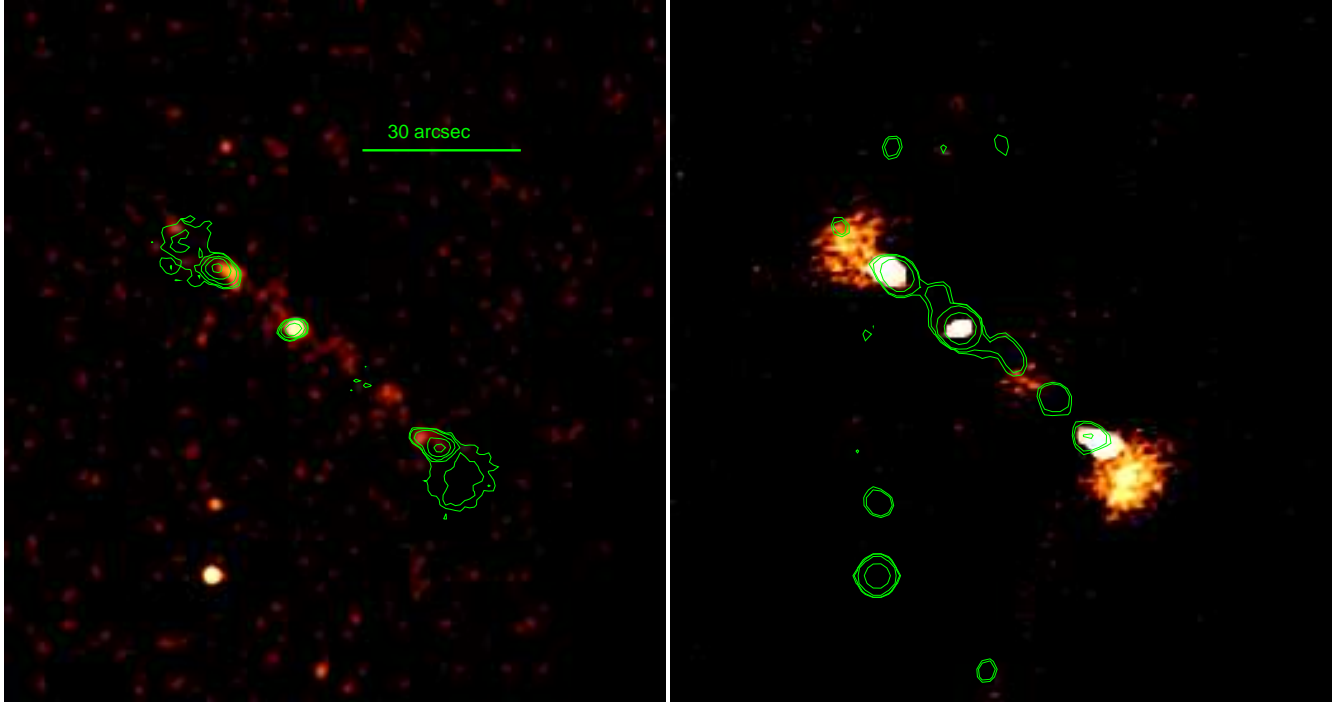


Figure 2. Left: overlay of 4.8 GHz contours on 0.5–3 keV X-ray colour-scale. Right: 0.5–3 keV X-rays, convolved with a Gaussian of 2.5 arcseconds, shown as contours overlaid on 4.8 GHz colour-scale.

2.2 Radio data

Data at 5 GHz had been observed by the VLA in its fairly extended B-configuration and its most compact D-configuration. These were retrieved from the archive under project codes AC234 and AR409 respectively and reduced separately using standard procedures within the AIPS software package including self-calibration for phases only. Confusing sources were subtracted from each UV-dataset using, sequentially, BOX2CC, CCEDT and UVSUB. The two datasets were concatenated, and cross-calibration was performed on the overlapping baselines between $0.5\text{ k}\lambda$ and $16\text{ k}\lambda$. The extended structure exterior to the hotspots was initially not included in any self-calibration model. The presence of this extended structure was robust to taking only half of the data at a time and seems to be a persistent and real feature of the brightness distribution. The north-east extended outer emission has a flux density of $8.4 \pm 0.1\text{ mJy}$ while that of the south-west extended outer emission has a flux density of $6.4 \pm 0.1\text{ mJy}$.

The integrated radio spectrum is plotted in Figure 3. Some of the datapoints are above the best-fit line but these correspond to survey measurements where often low-resolution and confusion overestimates the flux densities in what is a fairly clustered part of the radio sky. The radio spectrum is consistent with being a straight power-law following $\nu^{-1.1}$ up to frequencies of 1 GHz. The highest frequency points shown in the plot, at 5 GHz are (from top to bottom): our combined B+D configuration data, B-configuration data and below these are various surveys (Griffith et al. 1990; Gregory & Condon 1991). We suspect that the reason for these particular surveys apparently underestimating the flux density of this source compared with those obtained from pointed VLA observations is that only the south-west lobe of this arcminute-sized radio source is fitted in an automated manner by the surveys. With the extended spectral region described with a spectral index $\alpha = 1.1$, there is a (minimum) $\Delta\alpha \sim 0.5$ as inferred from the spectral index

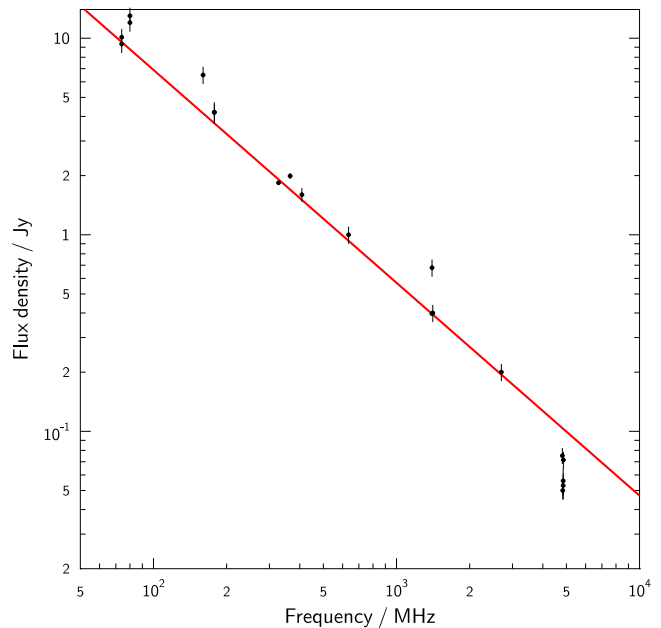


Figure 3. Spectrum of 4C23.56 at radio wavelengths; most datapoints are taken from NED, but those at 327 MHz and 4.7 GHz were taken from re-reduced radio data from the VLA archive. The line shown is fitted to all points with frequencies below 3 GHz and follows $\nu^{-1.1}$.

above 2.7 GHz to the 4.8 GHz data-point from our VLA measurements.

From the purely monochromatic radio view, as pointed out by Chambers et al. (1996), the two opposite lobes and the nucleus are perfectly co-linear although the length of the western arm is twice that of the eastern arm.

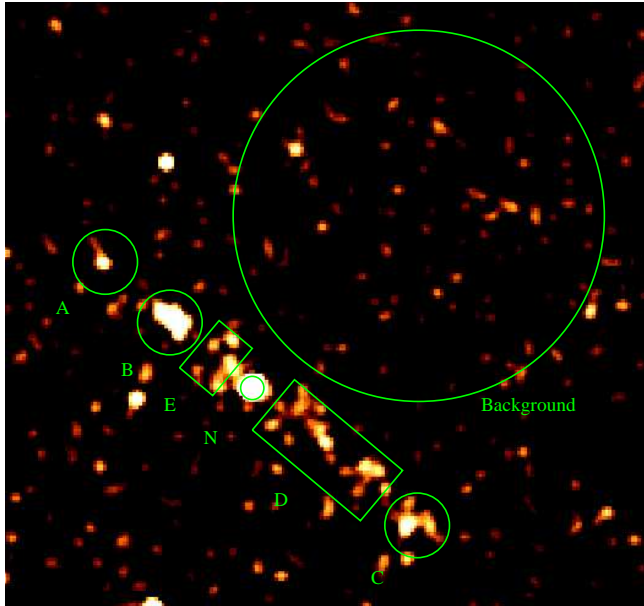


Figure 4. Illustration of the regions fitted from the X-ray observations to give the data presented in Table 1.

3 MAGNETIC FIELD ESTIMATE

An estimate of the magnetic field strength in the north-east inner radio tail (nearer the hotspot than the nucleus, shown in the NE inset to Fig 1) may be obtained by estimating the ratio of the co-spatial radio synchrotron luminosity with the ICCMB X-ray luminosity (Govoni & Feretti 2004). Care was taken to exclude the radio emission from the actual compact hotspot, which has no counterpart X-ray emission. With a radio flux density of 5 mJy and an X-ray flux density of $2.17 \times 10^{-15} \text{ erg cm}^{-2} \text{ s}^{-1}$, the magnetic field strength of this plasma is $16.2 \mu\text{G}$ (a.k.a. 1.62 nT). While this is an uncertain estimate, not least because of the assumption that the X-ray emission and radio synchrotron emission arise from the same particle population, which as described in Sec 4 is doubtful, it is an entirely plausible value consistent with other estimates of magnetic field strengths in the lobes of radio galaxies and quasars. In such a magnetic field strength, the particles responsible for the synchrotron emission at 5 GHz will have Lorentz factors of 1.03×10^4 , an order of magnitude more energetic than those responsible for inverse-Compton scattering CMB photons into X-ray photons. For comparison, the magnetic field strength may be estimated using minimum-energy assumptions Miley (e.g. 1980) for fiducial values of the lower limit of the energy distribution of the synchrotron particles, γ_{min} . As discussed by Blundell et al. (2006), the inferred magnetic field is lower for a higher assumed γ_{min} . Example values are: $218.2 \mu\text{G}$, $56.7 \mu\text{G}$, $28.9 \mu\text{G}$ and $16.0 \mu\text{G}$ for $\gamma_{\text{min}} = 1, 100, 1000, 7500$ respectively. We remind the reader that consistency seems to emerge on the basis of higher values of γ_{min} , the resolution of the radio/X-ray overlaid image could hide the fact that the X-ray emitting plasma and radio emitting plasma can only be assumed to be co-spatial.

4 EXTENDED X-RAY EMISSION IN THE OLDEST PARTS OF THE LOBES

Although the X-ray counts are slightly sparse across 4C23.56, luminosities and photon indices were obtained for regions A–E de-

Region	Luminosity ($\times 10^{44} \text{ erg s}^{-1}$)	Photon index
A	$0.32 \pm$	1.96 ± 0.82
B	1.29 ± 0.21	2.83 ± 0.50
C	$1.09 \pm$	2.28 ± 0.82
D	1.13 ± 0.20	2.79 ± 0.51
E	$0.73 \pm$	for fixed $\Gamma = 2$
E	1.1 ± 0.3	for fixed $\Gamma = 2.8$
N	$41.52 \pm$	2.27 ± 1.05

Table 1. Luminosities are measured between 2 and 10 keV in the rest frame and absorption corrected (both Galactic and intrinsic).

icted in Fig 4 (the nucleus is discussed separately in Sec 6). The photon indices fitted for the non-nuclear regions span a range of 2 – 2.8. This is broadly consistent with the value inferred by Johnson et al. (2007) of $\Gamma = 2.6$ for photon index of the lobe plasma although their observations from XMM, having lower angular resolution, would have been challenged by contamination from the nucleus. Although the Chandra photon indices are consistent with those inferred from the XMM measurements, they are inconsistent with the radio spectral index of $\alpha = 1.1$, which would for a single continuous power-law imply a photon index of $\Gamma = 2.1$. The radio synchrotron electrons are thus drawn from a harder (flatter) distribution than the electrons responsible for the ICCMB emission. We suggest that this points to a more recently accelerated population of electrons as the synchrotron population, than the older (‘spent’ synchrotron) lower energy electrons that upscatter CMB photons into the X-ray bands. This is consistent with the picture of a previous epoch of jet activity, whose only tell-tale sign is from relic ICCMB emission, and a current epoch of jet activity, evinced by radio synchrotron hotspots. We continue this line of thought in Sec 5 as we consider the unusual characteristic of the extended radio emission *external* to the hotspots in this powerful radio galaxy.

The most north-easterly source along the radio axis, delineated by Region A in Fig 4, has a colour, appearing as orange in Fig 1 which is clearly rare amongst the background sources. Its position, being almost exactly along the radio axis, and its colour resembling that of Region C suggests that it may be a part of the non-thermal emission associated with the jet activity of this object. The number of counts is however, too few to permit detailed analysis, other than (weakly) constraining its photon index or to securely identify its role (if any) within this active galaxy’s extended emission.

5 EXTENDED RADIO EMISSION BEYOND HOTSPOTS

The insets to Fig 1 clearly reveal how there is smooth radio emission *outside* of the hotspots, the regions of enhanced surface brightness which, usually in classical double FR II radio sources, are believed to be where the jets impinge and shock on the intergalactic medium. This outer emission is most uncharacteristic in powerful FR II radio sources. There appear to be no counterpart X-rays associated with this smooth emission, and it seems likely that X-rays would have been detected if they were there at the same level as the X-rays associated with the internal tails of the hotspots: the ratio of the X-ray counts in the tail region to the co-spatial, diffuse 4.9 GHz radio blob region (i.e. excluding the hotspot) as 13 to < 5.7 (2σ limit) i.e. > 2.3 , whereas the ratio of the radio fluxes for the same regions is 0.5. This means that we would have easily detected the external regions beyond the hotspots if they have the same electron

population as the tail regions. The external extended regions, lacking associated X-ray emission, therefore are deficient in $\gamma \sim 1000$ electrons compared with the internal tails. The radio emission in these regions is presumably synchrotron radiation and thus even the regions external to the hotspots require a magnetic field. Such external features are unknown in high- z , powerful radio sources which suggests that IGM magnetic field strengths are usually too low to be sufficient to “illuminate” the presence of high-energy electrons. Given the symmetry of these external extended features, we suggest that the most likely origin for the magnetic field responsible for this emission arises from pre-existing lobe plasma encountered by the outward moving radio hotspots, and possibly somewhat compressed by them. A weak magnetic field will illuminate high- γ electrons and if the deficiency in $\gamma \sim 1000$ particles is indeed real then this would strongly suggest that the turnover frequency in the energy spectrum of particles accelerated in the hotspot complexes is very significantly above 10^3 . We suggest that these high-energy particles leak out from the radio hotspot and, being ultra-relativistic, rapidly pervade the relic, expanded plasma having a very weak, but not necessarily tangled magnetic field. The extent to which ultra-relativistic electrons can pervade a pre-existing weakly-magnetized plasma may be described by a random walk of particles across randomly oriented regions of magnetic field (Rechester & Rosenbluth 1978). The efficacy of this transport mechanism depends critically on the configuration (tangling) of the magnetic field structure within the plasma which in turn depends on its original configuration and the geometry of any subsequent expansion. Anomalous diffusion mechanisms in plasma physics are currently not fully explored, but following Duffy et al. (1995) and assuming a tangling scale of 10 kpc (plausible for expanded lobe material often 10s of kpc across in spatial extent) then in 10^5 years the rms distance diffused is 10s of kpc, comparable with the extent of the external regions of plasma beyond the hotspots, as seen in the insets of Fig 1.

6 NUCLEUS, AND SUPPLY OF FUEL FOR A NEW EPISODE OF JET EJECTION

The absorption-corrected luminosity of 4C 23.56’s nucleus in the 2–10 keV band is 41.5×10^{44} erg s $^{-1}$ which for a typical quasar nucleus (e.g. Elvis et al. 1994) would make the total bolometric nuclear luminosity to be 2×10^{47} erg s $^{-1}$ and as such is one of the most energetic objects/nuclei in the universe. This luminosity is very close to the Eddington-limited luminosity for a supermassive black hole of a billion solar masses. Although recent research has suggested that objects with luminosities near the Eddington-limit tend not to have radio jets (e.g. Panessa et al. 2007; Sikora et al. 2007; Maoz 2007) 4C23.56, just like the other ~ 1 Mpc, $z \sim 2$ radio galaxy 6C0905+32 we studied (Erlund et al. 2008b), is another demonstrable counter-example. We note, however, that the Eddington limit is calculated with the simplifying, incorrect, assumption of spherical symmetry. The X-ray spectrum of this nucleus, shown in Fig 5 shows tentative evidence for a redshifted 6.4 keV iron line which is likely to be arise from the strong absorber.

The X-ray photon index of the nucleus, as listed in Table 1, is fitted to be $\Gamma = 2.27 \pm 1.05$. Though poorly constrained, it is interestingly consistent with the high-frequency radio spectral index of the nucleus, reported between 5 GHz and 15 GHz by Chambers et al. (1996) to be unusually steep at $\alpha = 1.44$. This is in contrast with the lower radio frequency spectral index of the nucleus of $\alpha = 0.62$.

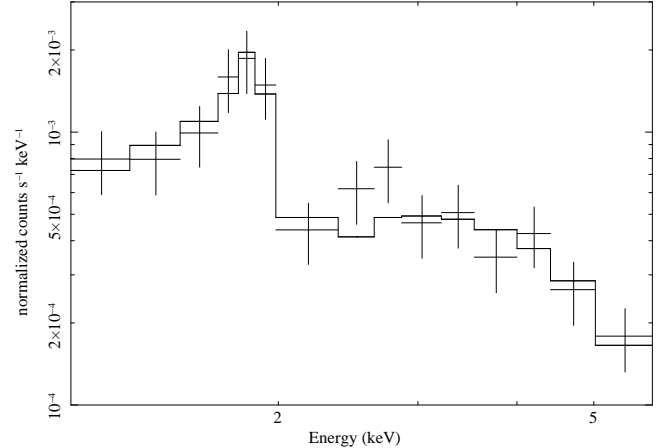


Figure 5. X-ray spectrum of the nucleus of 4C23.56 showing tentative evidence for a 6.4 keV iron line redshifted to $6.4/(1+z) = 1.8$ keV, just below the deep neutral iron K edge.

The nucleus of this powerful radio galaxy is highly obscured, having a column density of $0.79 \pm 0.5 \times 10^{24}$ cm $^{-2}$, slightly below the Compton-thick threshold of 1.5×10^{24} cm $^{-2}$ at which the Thomson-scattering optical depth reaches unity.

In the context of active nuclei that may be exhibiting multiple cycles of relativistic jet activity, Salter et al. (2010, and references therein) have pointed out that the presence of a higher than average amount of neutral hydrogen absorption seems to be associated with such “rejuvenated” or “re-activated” or multi-episodic radio galaxies. This characteristic appears to apply to sources of all sizes from compact to giant. Although we have no HI observations of 4C23.56 to bring to bear against the two strands of evidence that it has exhibited more than one episode of jet activity ([i] high-energy emission external to the hotspots requiring a pre-existing magnetic field and [ii] the harder synchrotron spectrum compared with that of the ICMB emission) there are two indications of a plentiful supply of gas in the vicinity of this nucleus: (i) the considerable column density of $0.79 \pm 0.5 \times 10^{24}$ cm $^{-2}$, (ii) the presence of two opposite cones, having $\sim 90^\circ$ opening angles, revealed in narrow-band Lyman- α imaging by Knopp & Chambers (1997) and presumably illuminated by ionising radiation from the nucleus and (iii) a rotating gas cloud with dynamical mass inferred from Keck spectroscopy by Villar-Martín et al. (2003) to be $2.9 \times 10^{12} M_\odot$.

We also note the remarkable structural asymmetry in this system: the SW arm is twice the length of the NE arm, and at half the distance along the SW arm there is some radio emission and an absence of X-ray emission (see Fig 2). Whether this corresponds to evidence of alternating activity in the opposite jets (“flip-flopping”) or to asymmetries induced by the presence of different plasma or other environmental differences is not clear with the present data, but follow-up observations will be sought from the eVLA.

7 DOUBLE SHOCK X-RAY/RADIO STRUCTURES AND PARTICLE ACCELERATION

Examination of the brightest peaks on the radio image, the compact hotspot peaks (see insets in Fig 1) reveals that the brightest compact radio hotspot peaks are offset from the brightest compact X-ray peaks in the same sense as each other: the X-ray hotspots are offset closer to the nucleus. This is in the same sense as in the unusually nearby and giant radio quasar 4C74.26 studied by

Erlund et al. (2010) (the offset in this object is 19 kpc projected on the plane of the sky) and for the quasar 4C19.44 (Sambruna et al. 2002) which has an offset of 14.5 kpc. 4C23.56 has a much larger offset of ~ 35 kpc; we note that the radio luminosity of 4C23.56 at $10^{28.22} \text{ W Hz}^{-1} \text{ sr}^{-1}$ is over three orders of magnitude higher than that of 4C74.26 at $10^{24.93} \text{ W Hz}^{-1} \text{ sr}^{-1}$. The origin of these offsets are still unclear but are explored in Erlund et al. (2010). A particular possibility we explore in that paper is that the shock nearer to the nucleus, (the X-ray peak) is from a population of high-energy electrons that cool radiatively as they flow downstream. A subsequent shock, further downstream, is where these cooled electrons are compressed and radiate in the radio.

8 CONCLUSIONS

This combined X-ray and radio study demonstrates a continuation of the pattern that X-ray shocks associated with hotspots appear to be upstream of the radio synchrotron shocks. Studies of other classical double radio sources have revealed evidence of previous epochs of jet ejection namely (i) double-double radio galaxies (e.g. Schoenmakers et al. 2000), (ii) the double-double X-ray/radio galaxies by (Laskar et al. 2010) and (iii) the presence of a relic X-ray counter-jet in the prototypical classical double radio galaxy, Cygnus A (Steenbrugge et al. 2008). In this study, of the giant (~ 0.5 Mpc) and high-redshift ($z \sim 2.5$) radio galaxy of 4C23.56, two strands of evidence have emerged that point to there being a previous episode of jet activity in this object other than the episode delineated by the current radio synchrotron emission. These strands of evidence are: (i) outside of the hotspots, further away from the nucleus, there is extended radio emission that may be plausibly explained by fast particles, freshly accelerated at the hotspots, leaking into pre-existing, weakly magnetised plasma that may be the relic lobes of a previous epoch of jet activity and (ii) the radio spectrum is considerably harder than that of the inverse-Compton emission. This argues against the emission being drawn from one single population of relativistic particles. A simple explanation for this is that the radio synchrotron is from more recently accelerated particles and the softer spectrum of the ICCMB emission corresponds to a previous episode of jet activity, that may even have been re-energized following compression because of the propagation of the current episode of jet ejection.

ACKNOWLEDGEMENTS

KMB and ACF thank the Royal Society. This research has made use of the NASA/IPAC Extragalactic Database (NED) which is operated by the Jet Propulsion Laboratory, California Institute of Technology, under contract with the National Aeronautics and Space Administration.

REFERENCES

Blundell, K. M., Fabian, A. C., Crawford, C. S., Erlund, M. C., & Celotti, A. 2006, *ApJ*, 644, L13
 Blundell K. M., Rawlings S., Willott C. J., 1999, *AJ*, 117, 677
 Carilli, C. L., Roettgering, H. J. A., van Ojik, R., Miley, G. K., & van Breugel, W. J. M. 1997, *ApJS*, 109, 1
 Chambers, K. C., Miley, G. K., van Breugel, W. J. M., Bremer, M. A. R., Huang, J.-S., & Trentham, N. A. 1996, *ApJS*, 106, 247
 Dickey J. M., Lockman F. J., 1990, *ARA&A*, 28, 215

Duffy, P., Kirk, J. G., Gallant, Y. A., & Dendy, R. O. 1995, *A&A*, 302, L21
 Elvis, M., et al. 1994, *ApJS*, 95, 1
 Erlund, M. C., Fabian, A. C., & Blundell, K. M. 2008, *MNRAS*, 386, 1774
 Erlund, M. C., Fabian, A. C., Blundell, K. M., & Crawford, C. S. 2008, *MNRAS*, 385, L125
 Erlund, M. C., Fabian, A. C., Blundell, K. M., Crawford, C. S., & Hirst, P. 2010, *MNRAS*, 404, 629
 Fanaroff B. L., Riley J. M., 1974, *MNRAS*, 167, 31P
 Fabian, A. C., Chapman, S., Casey, C. M., Bauer, F., & Blundell, K. M. 2009, *MNRAS*, 395, L67
 Govoni, F., & Feretti, L. 2004, *International Journal of Modern Physics D*, 13, 1549
 Gregory, P. C., & Condon, J. J. 1991, *ApJS*, 75, 1011
 Griffith, M., Langston, G., Heflin, M., Conner, S., Lehar, J., & Burke, B. 1990, *ApJS*, 74, 129
 Kalberla, P. M. W., Burton, W. B., Hartmann, D., Arnal, E. M., Bajaja, E., Morras, R., Pöppel, W. G. L. 2005, *A&A*, 440, 775
 Knopp, G. P., & Chambers, K. C. 1997, *ApJS*, 109, 367
 Laskar, T., Fabian, A. C., Blundell, K. M., & Erlund, M. C. 2010, *MNRAS*, 401, 1500
 Johnson, O., Almaini, O., Best, P. N., & Dunlop, J. 2007, *MNRAS*, 376, 151
 Maoz, D. 2007, *MNRAS*, 377, 1696
 Miley, G. 1980, *ARA&A*, 18, 165
 Mocz, P., Fabian, A.C. & Blundell, K.M., 2010, *MNRAS* submitted; arXiv:1008.2188
 Panessa, F., Barcons, X., Bassani, L., Cappi, M., Carrera, F. J., Ho, L. C., & Pellegrini, S. 2007, *A&A*, 467, 519
 Rechester, A. B., & Rosenbluth, M. N. 1978, *Physical Review Letters*, 40, 38
 Roettgering, H. J. A., van Ojik, R., Miley, G. K., Chambers, K. C., van Breugel, W. J. M., & de Koff, S. 1997, *A&A*, 326, 505
 Salter, C. J., Saikia, D. J., Minchin, R., Ghosh, T., & Chandola, Y. 2010, *ApJ*, 715, L117
 Sambruna, R. M., Maraschi, L., Tavecchio, F., Urry, C. M., Cheung, C. C., Chartas, G., Scarpa, R., & Gambill, J. K. 2002, *ApJ*, 571, 206
 Schoenmakers, A. P., de Bruyn, A. G., Röttgering, H. J. A., van der Laan, H., & Kaiser, C. R. 2000, *MNRAS*, 315, 371
 Sikora, M., Stawarz, Ł., & Lasota, J.-P. 2007, *ApJ*, 658, 815
 Steenbrugge, K. C., Blundell, K. M., & Duffy, P. 2008, *MNRAS*, 388, 1465
 Villar-Martín, M., Vernet, J., di Serego Alighieri, S., Fosbury, R., Humphrey, A., & Pentericci, L. 2003, *MNRAS*, 346, 273